Two-band superfluidity from the BCS to the BEC limit

M. Iskin and C. A. R. Sá de Melo
School of Physics, Georgia Institute of Technology, Atlanta, Georgia 30332, USA
(Received 22 March 2006; revised manuscript received 18 July 2006; published 25 October 2006)

We analyze the evolution of two-band superfluidity from the Bardeen-Cooper-Schrieffer (BCS) to the Bose-Einstein condensation (BEC) limit. When the interband interaction is tuned from negative to positive values, a quantum phase transition occurs from a 0-phase to a π-phase state, depending on the relative phase of the two order parameters. Furthermore, population imbalances between the two bands can be created by tuning the intraband or interband interactions. We also find two undamped low-energy collective excitations corresponding to in-phase and out-of-phase modes. Lastly, we derive the coupled Ginzburg-Landau equations, and show that they reduce to coupled Gross-Pitaevskii equations for two types of bosons in the BEC limit.

DOI: 10.1103/PhysRevB.74.144517 PACS number(s): 74.20.Fg, 05.30.Fk, 03.75.Hh, 03.75.Ss

I. INTRODUCTION

The evolution from the Bardeen-Cooper-Schrieffer (BCS) state to Bose-Einstein condensation (BEC) is a very important topic of current research in the condensed matter, nuclear, atomic, and molecular physics communities.[1–7] In atomic physics, the BCS to BEC evolution is studied via Feshbach resonances[8–17] in engineered one-band fermion systems involving two hyperfine states of alkali-metal atoms such as ^{6}Li or ^{40}K. However, two-band fermion systems may also be produced experimentally with ultracold atomic Fermi gases in optical lattices[17] or in single traps of several hyperfine states. In this case, (intraband and interband) interactions may be tuned using Feshbach resonances which allow for the study of BCS to BEC evolution of two-band superfluidity. This evolution in the two-band problem is much richer than the one-band case (where a smooth crossover of physical properties has been experimentally found[8–13]), since additional interaction parameters may be controlled externally.

An early two-band theory of superconductivity was introduced to allow for multiple band crossings at the Fermi surface.[18] This theory and its extensions are strictly limited to the BCS regime, and they have been applied to MgB_2, where experimental properties can be well described by a two-band BCS theory.[19–22] Unfortunately, interband or intraband interactions cannot be tuned in MgB_2, and presently its physical properties cannot be studied away from the BCS limit. However, new experimental techniques utilizing the field effect[23] may allow some tuning of the particle density and thus indirectly the tuning of interactions. In contrast, ultracold fermions with several hyperfine states may already provide a unique opportunity to explore new phenomena in two-band superfluids during the BCS to BEC evolution. Thus, due to recent developments and advances in atomic physics described above, and in anticipation of future experiments, we describe here the BCS to BEC evolution of two-band superfluids at zero and finite temperatures.

The main results of our paper are as follows. We show that a quantum phase transition occurs from a 0-phase to a π-phase state depending on the relative phase of the two order parameters, when the interband interaction is tuned from negative to positive values. We found that population imbalances between the two bands can be created by tuning intraband or interband interactions. In addition, we describe the evolution of two undamped low-energy collective excitations corresponding to in-phase phonon (Goldstone) and out-of-phase exciton (finite frequency) modes. Near the critical temperature, we derive the coupled Ginzburg-Landau (GL) equations, and show that they reduce to coupled Gross-Pitaevskii (GP) equations for two types of bosons in the BEC limit.

II. TWO-BAND MODEL

To obtain the results mentioned above, we start from a two-band Hamiltonian describing continuum superfluids with singlet pairing,

$$H = \sum_{n,\mathbf{k},\sigma} \xi_n(\mathbf{k}) a^\dagger_{n,\sigma}(\mathbf{k}) a_{n,\sigma}(\mathbf{k}) - \sum_{n,m,\mathbf{q}} V_{nm} b^\dagger_n(\mathbf{q}) b_m(\mathbf{q}), \quad (1)$$

where $\{n,m\}=\{1,2\}$ label different bands, and σ labels spins (or pseudospins). The operators $a^\dagger_{n,\uparrow}(\mathbf{k})$ and $b^\dagger_n(\mathbf{q}) = \Sigma_{\mathbf{k}} \Gamma^*_n(\mathbf{k}) a^\dagger_{n,\uparrow}(\mathbf{k}+\mathbf{q}/2) a^\dagger_{n,\downarrow}(-\mathbf{k}+\mathbf{q}/2)$ create a single and a pair of fermions, respectively. The symmetry factor $\Gamma_n(\mathbf{k})$ characterizes the chosen angular momentum channel, where $\Gamma_n(\mathbf{k}) = k_{n,0}/\sqrt{k^2_{n,0}+k^2}$ is for the s-wave interaction in three dimensions. Here, $k_{n,0} \sim R^{-1}_{n,0}$ sets the scale at small and large momenta, where $R_{n,0}$ plays the role of the interaction range. In addition $\xi_n(\mathbf{k}) = \epsilon_n(\mathbf{k}) - \mu_n$, where $\epsilon_n(\mathbf{k}) = \varepsilon_{n,0} + k^2/(2M_n)$ is the kinetic energy ($\hbar=1$) and M_n is the effective band mass of the fermions.

From now on, we focus on a two-band system with distinct intraband ($V_{11}, V_{22} > 0$) and interband ($V_{12}=V_{21}=J$) interactions. Notice that we allow pairing between states $|1,\uparrow\rangle$ and $|1,\downarrow\rangle$ or $|2,\uparrow\rangle$ and $|2,\downarrow\rangle$, and that pairing between $|1,\uparrow\rangle$ and $|2,\downarrow\rangle$ or $|1,\downarrow\rangle$ and $|2,\uparrow\rangle$ is not included. Here, $|n,\sigma\rangle$ represents a spin component with band index n and pseudospin σ. Furthermore, notice that J plays the role of the Josephson interaction which couples the two energy bands. In addition, we assume that the total number of fermions N is fixed such that $\mu_n = \mu$, and that the reference energies are such that $\varepsilon_{1,0}=0$ and $\varepsilon_{2,0}=\epsilon_D \geq 0$. Here, $\epsilon_D \ll \epsilon_{2,F}$ where $\epsilon_{n,F} = k^2_{n,F}/(2M_n)$ is the Fermi energy ($\epsilon_{1,F} \geq \epsilon_{2,F}$), and $k_{n,F}$ is the Fermi momenta [see Fig. 1(a)]. In addition, notice that $k_{n,0} \gg k_{n,F}$ in dilute systems.

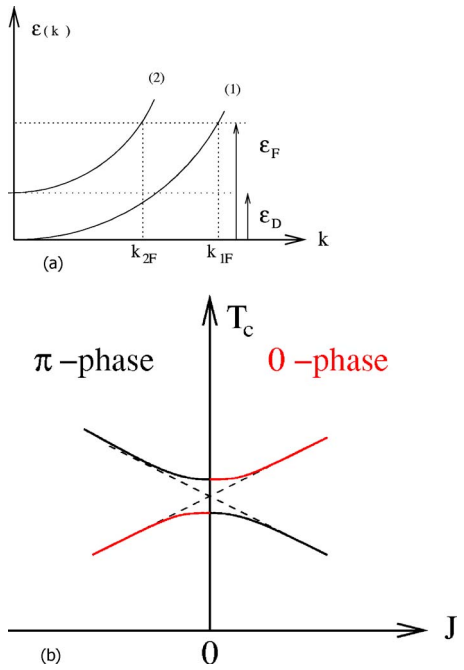

FIG. 1. (Color online) Schematic (a) figure of two bands with reference energies $\varepsilon_{1,0}=0$ and $\varepsilon_{2,0}=\epsilon_D$, and (b) phase diagram of 0-phase and π-phase states.

We would like to emphasize that the model Hamiltonian described in Eq. (1) may be applicable to atomic and condensed matter systems. The case of identical bands ($M_1=M_2=M$) corresponds physically to a situation that may be encountered in atomic systems when four hyperfine states of a given type of atom (labeled as $|1,\uparrow\rangle$; $|1,\downarrow\rangle$; $|2,\uparrow\rangle$; $|2,\downarrow\rangle$) are trapped. In this case, the Josephson terms are responsible for transferring pairs of atoms between states $|1,\uparrow;1,\downarrow\rangle$ and $|2,\uparrow;2,\downarrow\rangle$, and thus mixing different bands. Notice that the case of nonidentical bands ($M_1\neq M_2$) is not applicable to mixtures of two atomic species (e.g., ^{6}Li and ^{40}K), because the Josephson term would convert Li pairs into K pairs, which is not physically allowed. However, the case of nonidentical bands may be applicable to standard condensed matter systems such as MgB_2, since electrons may have different effective masses in different bands, and the Josephson term is physically allowed. In Sec. V, we discuss a generalized two-band model that includes the case of nonidentical masses for atomic systems.

A. Effective action

The Gaussian action for the Hamiltonian H (in units of $k_B=1, \beta=1/T$) is $S_{\text{Gauss}}=S_0+(\beta/2)\Sigma_q\Lambda^\dagger(-q)\mathbf{F}^{-1}(q)\Lambda(q)$, where $q=(\mathbf{q}, iv_\ell)$ denotes both momentum and bosonic Matsubara frequency $v_\ell=2\ell\pi/\beta$. Here, the vector $\Lambda^\dagger(-q)$ is the order parameter fluctuation field, and the matrix $\mathbf{F}^{-1}(q)$ is the inverse fluctuation propagator. The saddle point action is

$$S_0=\sum_{n,\mathbf{k}}\{\beta[\xi_n(\mathbf{k})-E_n(\mathbf{k})]-2\ln[1+e^{-\beta E_n(\mathbf{k})}]\}$$
$$-\beta\sum_{n,m}g_{nm}\Delta_{n,0}^*\Delta_{m,0}, \tag{2}$$

where $E_n(\mathbf{k})=[\xi_n^2(\mathbf{k})+|\Delta_n(\mathbf{k})|^2]^{1/2}$ is the energy of the quasiparticles and $\Delta_n(\mathbf{k})=\Delta_{n,0}\Gamma_n(\mathbf{k})$ is the order parameter. Here, the matrix elements of $\mathbf{g}$ are associated with the inverse interaction matrix $\mathbf{V}$, and are given by $g_{11}=-V_{22}/\det\mathbf{V}$, $g_{22}=-V_{11}/\det\mathbf{V}$, and $g_{12}=g_{21}=J/\det\mathbf{V}$ with $\det\mathbf{V}=V_{11}V_{22}-J^2>0$.

The action leads to the thermodynamic potential $\Omega_{\text{Gauss}}=\Omega_0+\Omega_{\text{fluct}}$, where $\Omega_0=S_0/\beta$ is the saddle point and $\Omega_{\text{fluct}}=(1/\beta)\Sigma_q\ln\det[\mathbf{F}^{-1}(q)/(2\beta)]$ is the fluctuation contribution to Ω_{Gauss}. Expressing $\Delta_{n,0}$ in terms of its amplitude and phase

$$\Delta_{n,0}=|\Delta_{n,0}|\exp(i\varphi_n) \tag{3}$$

shows explicitly the Josephson coupling energy

$$-g_{11}|\Delta_{1,0}|^2-g_{22}|\Delta_{2,0}|^2-2g_{12}|\Delta_{1,0}\Delta_{2,0}|\cos(\varphi_2-\varphi_1)$$

of Ω_0. When $J>0$, only the 0-phase (or in-phase) $\varphi_2=\varphi_1$ solution is stable. However, when $J<0$, only the π-phase (or out-of-phase) $\varphi_2=\varphi_1+\pi$ solution is stable. Thus, a phase transition occurs from the 0 phase to the π phase when the sign of J is tuned from negative to positive values as shown in Fig. 1(b).

B. Self-consistency equations

From the stationary condition $\partial S_0/\partial\Delta_n^*(q)=0$, we obtain the order parameter equation

$$\begin{pmatrix}O_{11} & O_{12}\\ O_{21} & O_{22}\end{pmatrix}\begin{pmatrix}\Delta_{1,0}\\ \Delta_{2,0}\end{pmatrix}=0, \tag{4}$$

where the matrix elements are given by $O_{nm}=-g_{nm}-\delta_{nm}\Sigma_{\mathbf{k}}|\Gamma_m(\mathbf{k})|^2\tanh[\beta E_m(\mathbf{k})/2]/[2E_m(\mathbf{k})]$. Here, δ_{nm} is the Kronecker delta. The order parameter equations can also be written in a more familiar form as

$$\Delta_{n,0}=\sum_{m,\mathbf{k}}\frac{V_{nm}\Delta_{m,0}|\Gamma_m(\mathbf{k})|^2}{2E_m(\mathbf{k})}\tanh\frac{\beta E_m(\mathbf{k})}{2}. \tag{5}$$

Notice that the order parameter amplitudes are the same for both the 0 and π phases as can be shown directly from Eq. (4), but their relative phases are either 0 or π. In what follows, we analyze only the 0-phase state, keeping in mind that analogous results (with appropriate relative phase changes) apply to the π-phase state. We can eliminate V_{nn} in favor of scattering length a_{nn} via the relation

$$\frac{1}{V_{nn}}=-\frac{M_n\mathcal{V}}{4\pi a_{nn}}+\sum_{\mathbf{k}}\frac{|\Gamma_n(\mathbf{k})|^2}{2\epsilon_n(\mathbf{k})}, \tag{6}$$

where $\mathcal{V}$ is the volume. This relation can be rewritten as

$$\frac{2}{\lambda_{nn}}=\pi\sqrt{\frac{\epsilon_{n,0}}{\epsilon_{n,F}}}-\frac{\pi}{k_{n,F}a_{nn}}, \tag{7}$$

where $\epsilon_{n,0}=k_{n,0}^2/(2M_n)$, and $\lambda_{nm}=V_{nm}D_m$ are the dimensionless interaction parameters with $D_m=M_m\mathcal{V}k_{m,F}/(2\pi^2)$ being the density of states per spin (pseudospin) of noninteracting fermions at the Fermi energy.

The order parameter equation needs to be solved self-consistently with the number equation $N=-\partial\Omega/\partial\mu$ leading to $N_{\text{Gauss}}=N_0+N_{\text{fluct}}$, and is given by

$$N_{\mathrm{Gauss}} = \sum_{\mathbf{k},\sigma,n} \mathcal{N}_{0,n}(\mathbf{k}) - \frac{1}{\beta}\sum_{q} \frac{\partial[\det \mathbf{F}^{-1}(q)]/\partial\mu}{\det \mathbf{F}^{-1}(q)}. \quad (8)$$

Here, the first term is the saddle point (N_1+N_2) and the second term is the fluctuation (N_{fluct}) contribution, where $\mathcal{N}_{0,n}=1/2-\xi_n(\mathbf{k})\tanh[\beta E_n(\mathbf{k})/2]/[2E_n(\mathbf{k})]$ is the momentum distribution. The inclusion of N_{fluct} is very important near the critical temperature, however, N_0 may be sufficient at low temperatures.[4,5]

In the remainder of the paper, numerical results are given only for identical bands $(M_1=M_2=M)$ with zero offset $(\epsilon_D=0)$, which correspond physically to situations that may be encountered in atomic physics when four hyperfine states of a given atomic system are trapped. However, we also present analytical results for the case of unequal band masses, which may be applicable to standard condensed matter systems such as MgB_2. In this case, the particle density may be tuned using field effect techniques,[23] and it may be possible to study two-band systems away from the higher-density (weakly interacting) BCS regime toward the lower-density (strongly interacting) BEC regime.

III. ZERO TEMPERATURE

In this section, we analyze the saddle point order parameter amplitudes $|\Delta_{n,0}|$ and the chemical potential μ at $T=0$. We first obtain analytical results in the strictly BCS and BEC limits, and then perform numerical calculations in the evolution from BCS to BEC, which are discussed next.

A. Saddle point: BCS and BEC limits

In the strictly BCS and BEC limits, the self-consistent (order parameter and number) equations are decoupled, and play reversed roles. In the BCS (BEC) limit, the order parameter equations determine $|\Delta_{n,0}|$ (μ), and the number equation determines μ $(|\Delta_{n,0}|)$.

The BCS limit is characterized by a positive chemical potential with respect to the bottom of the fermion band $\mu>0$ and $\max\{|\Delta_{1,0}|,|\Delta_{2,0}|\}\ll\epsilon_{2,F}$, where pairing occurs between the fermions whose energy are close to $\epsilon_{1,F}$. In this limit, the solutions of the order parameter equation are

$$\max\{|\Delta_{1,0}|,|\Delta_{2,0}|\} \sim 8\epsilon_F \exp[-2+\pi\sqrt{\epsilon_0/(4\epsilon_F)}-\phi_-]$$

for the larger of the order parameter amplitudes and

$$\min\{|\Delta_{1,0}|,|\Delta_{2,0}|\} \sim 8\epsilon_F \exp[-2+\pi\sqrt{\epsilon_0/(4\epsilon_F)}-\phi_+]$$

for the smaller of the order parameter amplitudes, while the number equation leads to $\mu\approx\epsilon_F$. Here, $\phi_\pm=\lambda_+\pm[\lambda_+^2-1/\det\lambda]^{1/2}$ where $\lambda_\pm=(\lambda_{11}\pm\lambda_{22})/(2\det\lambda)$, $\det\lambda=\lambda_{11}\lambda_{22}-\lambda_{12}\lambda_{21}$, and we assumed $\epsilon_{1,F}\sim\epsilon_{2,F}=\epsilon_F$ and $\epsilon_{1,0}\sim\epsilon_{2,0}=\epsilon_0$. The familiar one-band results are again recovered when $J\to0$ leading to $|\Delta_{n,0}|\sim8\epsilon_{n,F}\exp[-2+\pi\sqrt{\epsilon_{n,0}/(4\epsilon_{n,F})}-1/\lambda_{nn}]$ for the order parameters and $\mu=\epsilon_{n,F}$ for the chemical potentials. The previous expression can be simplified by using Eq. (7), leading to $|\Delta_{n,0}|=8\epsilon_{n,F}\exp[-2+\pi/(2k_{n,F}a_{nn})]$, which is the standard one-band result.[5]

On the other hand, the BEC limit is characterized by negative chemical potential with respect to the bottom of the lowest band $\mu<0$ and $\max\{|\Delta_{1,0}|,|\Delta_{2,0}|\}\ll|\mu|\ll\epsilon_0$, where pairing occurs between all fermions. In this limit, the solution of the order parameter equations is

$$\mu_\pm = -\epsilon_0[\pi\sqrt{\epsilon_0/(4\epsilon_F)}/\phi_\pm - 1]^2,$$

while the number equation leads to

$$|\Delta_{n,0}|^2 = (8\pi\mathcal{N}_n/M_n)\sqrt{|\mu|/(2M_n)}.$$

Here, $\mathcal{N}_n=N_n/\mathcal{V}$ is the density of the fermions in band n. Notice that the total density of fermions is $\mathcal{N}=\mathcal{N}_1+\mathcal{N}_2=(k_{1,F}^3+k_{2,F}^3)/(3\pi^2)$. The familiar one-band results are again recovered when $J\to0$ leading to $\mu_n=-\epsilon_{n,0}[\pi\lambda_{nn}\sqrt{\epsilon_{n,0}/(4\epsilon_{n,F})}-1]^2$ for the chemical potentials,[3] which can be written in terms of the scattering lengths[5] as $\mu_n=-1/(2M_na_{nn}^2)$, using Eq. (7), and the condition $k_{n,0}a_{nn}\gg1$. The one-band order parameter amplitudes are also given by $|\Delta_{n,0}|^2=16\epsilon_{n,F}^2\sqrt{|\mu_n|/\epsilon_{n,F}}/(3\pi)$, where we used $\mathcal{N}_n=k_{n,F}^3/(3\pi^2)$.

B. Saddle point: BCS to BEC evolution

Next, we analyze numerically the evolution of the order parameter amplitudes and the chemical potential from the BCS to the BEC limit for identical bands $(M_1=M_2=M)$ with zero offset $(\epsilon_D=0)$ at zero temperature. For this purpose, we solve the coupled self-consistency equations Eqs. (5) and (8), for parameters $k_{1,0}=k_{2,0}=k_0\approx256k_F$ and $V_{22}=0.001$ in units of $5.78/(Mk_F\mathcal{V})$ [or $1/(k_Fa_{22})\approx-3.38$], and analyze two cases.

In the first case, we solve for μ, $|\Delta_{1,0}|$ and $|\Delta_{2,0}|$ as a function of V_{11} [or $1/(k_Fa_{11})$], and show $\Delta_{n,0}$ in Fig. 2(a) for fixed values of J. The unitarity limit is reached at $V_{11}\approx1.0132V_{22}$ [or $1/(k_F|a_{11}|)\approx0$] while μ changes sign at $V_{11}\approx1.0159V_{22}$ [or $1/(k_Fa_{11})\approx0.69$]. The evolution of $|\Delta_{1,0}|$ is similar to the one-band result[4] where it grows monotonically with increasing V_{11}. However, the evolution of $|\Delta_{2,0}|$ is nonmonotonic having a hump at approximately $V_{11}\approx1.0155V_{22}$ [or $1/(k_Fa_{11})\approx0.58$], and it decreases for stronger interactions until it vanishes (not shown). In the case of ultracold atoms, the order parameter may be measured using similar techniques as for one-band systems[14] involving only ^{6}Li. In Fig. 2(b), we show that both bands have similar populations for $V_{11}\sim V_{22}$. However, as V_{11}/V_{22} increases, fermions from the second band are transferred to the first, where bound states are easily formed and reduce the free energy. In coupled two-band systems, spontaneous population imbalances are induced by the increasing scattering parameter (interaction) in contrast with the one-band case, where population imbalances are prepared externally.[15,16]

In the second case, we solve for μ, $|\Delta_{1,0}|$, and $|\Delta_{2,0}|$ as functions of J, and show μ in Fig. 3(a) and band populations N_n in Fig. 3(b) for fixed values of V_{11}/V_{22}. The order parameters $|\Delta_{1,0}|$ and $|\Delta_{2,0}|$ grow with increasing J (not shown). Notice the population imbalance and the presence of maxima (minima) in N_1 (N_2) for finite J, which is associated with the sign change of μ shown in Fig. 3(a). When $V_{11}>V_{22}$, there is

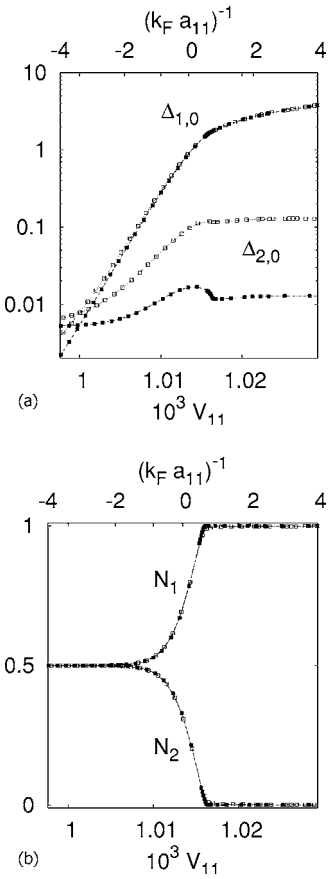

FIG. 2. Plots of (a) order parameter amplitude $|\Delta_{n,0}|$ (in units of ϵ_F), and (b) fraction of fermions N_n/N versus V_{11} [in units of $5.78/(Mk_F\mathcal{V})$] and versus $1/(k_Fa_{11})$ for $J=0.001V_{22}$ (hollow squares) and $J=0.0001V_{22}$ (solid squares).

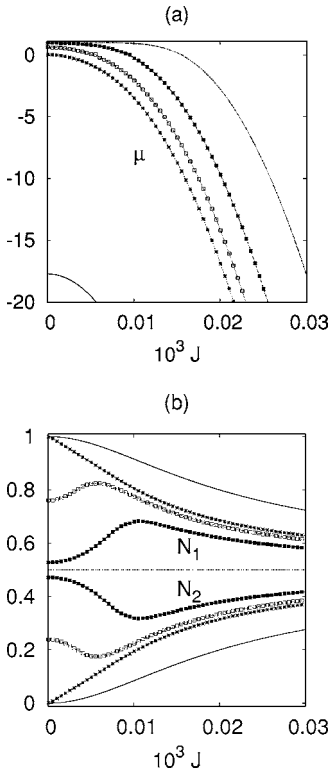

FIG. 3. Plots of (a) chemical potential μ (in units of ϵ_F), and (b) fraction of fermions N_n/N versus J [in units of $5.78/(Mk_F\mathcal{V})$] for $V_{11}=\gamma V_{22}$ where $\gamma=1$ (dotted lines), 1.010 (solid squares), 1.014 (hollow squares), 1.016 (crossed lines), and 1.030 (solid lines); or $1/(k_Fa_{11})\approx -3.38, -0.81$, 0.20, 0.70, and 4.17, respectively.

population imbalance even for $J=0$, because atom pairs can be easily transferred from the second band to the first until an optimal J_0 is reached. Further increase in J produces also transfer from the first band to the second, leading to similar populations for $J \gg J_0$. Therefore, the Josephson coupling parameter J acts as a knob to tune the populations of bands 1 and 2.

C. Collective Excitations

Next, we discuss the low-energy collective excitations at $T=0$, which are determined by the poles of the propagator matrix $\mathbf{F}(q)$ for the pair fluctuation fields $\Lambda_n(q)$, which describe the Gaussian deviations about the saddle point order parameter. The poles of $\mathbf{F}(q)$ are determined by the condition $\det \mathbf{F}^{-1}(q)=0$, which leads to collective (amplitude and phase) modes, when the usual analytic continuation $iv_\ell \rightarrow w+i0^+$ is performed. The easiest way to get the phase collective mode is to integrate out the amplitude field to obtain a phase-only effective action. Notice that a well-defined low-frequency expansion is possible only at $T=0$ for s-wave systems, due to Landau damping present at finite temperatures, causing the collective modes to decay into the two-quasiparticle continuum.

The phase-only collective excitations in the BCS and BEC limits lead to a Goldstone mode $w^2(\mathbf{q})=v^2|\mathbf{q}|^2$ characterized by the speed of sound,

$$v^2=(D_1v_1^2+D_2v_2^2)/(D_1+D_2),$$

and a finite-frequency mode $w^2(\mathbf{q})=w_0^2+u^2|\mathbf{q}|^2$ characterized by the finite frequency

$$w_0^2=4\alpha|g_{12}\Delta_{1,0}\Delta_{2,0}|\sqrt{\epsilon_F/|\mu|}(D_1+D_2)/(D_1D_2)$$

and the speed

$$u^2=(D_1v_2^2+D_2v_1^2)/(D_1+D_2).$$

In the BCS limit, $\alpha=1$ and $v_n=v_{n,F}/\sqrt{3}$, while $\alpha=1/\pi$ and $v_n=|\Delta_{n,0}|/\sqrt{8M_n|\mu|}$ in the BEC limit. Here, $v_{n,F}$ is the Fermi velocity. Here, we assumed $\epsilon_{1,F}\sim\epsilon_{2,F}=\epsilon_F$ and $k_{n,0}/k_{n,F}\rightarrow\infty$. The familiar one-band results are again recovered when $J\rightarrow 0$ leading to $v=v_1$, and $w_0=0$ and $u=v_2$.

It is also illustrative to analyze the eigenvectors associated with these solutions in the BCS and BEC limits. In the limit of $\mathbf{q}\rightarrow\mathbf{0}$, we obtain

$$(\theta_1,\theta_2)\propto(|\Delta_{1,0}|,|\Delta_{2,0}|)$$

for the Goldstone mode corresponding to an in-phase solution, while we obtain

$$(\theta_1,\theta_2) \propto (D_2|\Delta_{1,0}|,-D_1|\Delta_{2,0}|)$$

for the finite-frequency (exciton) mode corresponding to an out-of-phase solution. Notice that, in the case of identical bands with zero offset and identical order parameter amplitudes, the collective mode simplifies to be perfectly in phase where $(\theta_1,\theta_2)\propto(1,1)$, and perfectly out of phase where $(\theta_1,\theta_2)\propto(1,-1)$. These in-phase and out-of-phase collective modes are associated with the in-phase and out-of-phase fluctuations of the order parameters around their saddle point values, respectively. Our findings generalize Leggett's BCS results.[24,25] Notice that measurements of collective modes are already possible in one-band atomic systems,[26,27] but the two-band problem provides an additional richness which is the existence of the finite-frequency (Leggett) mode in addition to the low-frequency (Goldstone) mode.

IV. FINITE TEMPERATURES

Next, we discuss two-band superfluidity near the critical temperature T_c, where $|\Delta_{1,0}|\sim|\Delta_{2,0}|\to 0$. Our basic motivation here is to investigate the low-frequency and long-wavelength behavior of the order parameter near T_c. For $T=T_c$, the order parameter equation reduces to

$$\det\mathbf{O} = O_{11}O_{22} - O_{12}O_{21} = 0, \tag{9}$$

and the saddle point number equation $N_0=\Sigma_{\mathbf{k},\sigma,n}n_F[\xi_n(\mathbf{k})]$ corresponds to the number of unbound fermions, where $n_F(x)=1/[\exp(\beta x)+1]$ is the Fermi distribution. While N_0 is sufficient in the BCS limit, the inclusion of $N_{\rm fluct}$ is crucial in the BEC limit to produce the qualitatively correct physics, and can be obtained as follows.

A. Fluctuations near T_c

Near $T=T_c$, the fluctuation action $S_{\rm fluct}$ reduces to $S_{\rm fluct}=\beta\Sigma_{q,n,m}L^{-1}_{nm}(q)\Lambda^*_n(q)\Lambda_m(q)$ where

$$L^{-1}_{nn} = -g_{nn} - \sum_{\mathbf{k}} \frac{1-n_F(\xi_{n+})-n_F(\xi_{n-})}{\xi_{n+}+\xi_{n-}-iv_\ell}|\Gamma_n(\mathbf{k})|^2 \tag{10}$$

corresponds to the fluctuation propagator of band n, $L^{-1}_{n\neq m}(q)=g_{nm}$, and $\xi_{n\pm}=\xi_n(\mathbf{k}\pm\mathbf{q}/2)$. Thus, the resulting action leads to $\Omega_{\rm fluct}=(1/\beta)\Sigma_q \ln[\det\mathbf{L}^{-1}(q)/\beta^2]$, where $\det\mathbf{L}^{-1}(q)=L^{-1}_{11}(q)L^{-1}_{22}(q)-g_{12}g_{21}$. Notice that $\det\mathbf{L}^{-1}(0)=0$ also produces Eq. (9), which is the Thouless condition. After the analytic continuation $iv_\ell\to w+i0^+$, we expand $L^{-1}_{nn}(q)$ to first order in w and second order in $\mathbf{q}$ such that

$$L^{-1}_{nn}(q) = a_n + \sum_{i,j}\frac{c^{ij}_n}{2M_n}q_iq_j - d_nw. \tag{11}$$

The zeroth-order coefficient $L^{-1}_{nn}(0,0)$ is given by

$$a_n = -g_{nn} - \sum_{\mathbf{k}}\frac{X_n}{2\xi_n(\mathbf{k})}|\Gamma_n(\mathbf{k})|^2, \tag{12}$$

where $X_n=\tanh[\beta\xi_n(\mathbf{k})/2]$. The second-order coefficient $c^{ij}_n=M_n\partial^2L^{-1}_{nn}(\mathbf{q},0)/(\partial q_i\partial q_j)$ evaluated at $\mathbf{q}=\mathbf{0}$ is given by

$$c^{ij}_n = \sum_{\mathbf{k}}\left[\left(\frac{X_n}{8\xi^2_n(\mathbf{k})}-\frac{\beta Y_n}{16\xi_n(\mathbf{k})}\right)\delta_{ij}+\frac{\beta^2X_nY_n}{16M_n\xi_n(\mathbf{k})}k_ik_j\right]|\Gamma_n(\mathbf{k})|^2, \tag{13}$$

where $Y_n=\mathrm{sech}^2[\beta\xi_n(\mathbf{k})/2]$ and δ_{ij} is the Kronecker delta. Notice that $c^{ij}_n=c_n\delta_{ij}$ is isotropic for the s wave considered here. The coefficient d_n has real and imaginary parts, and for the s-wave case is given by

$$d_n = \sum_{\mathbf{k}}\frac{X_n}{4\xi^2_n(\mathbf{k})}|\Gamma_n(\mathbf{k})|^2 + i\frac{\beta\pi D_n\epsilon_{n,0}}{8(\epsilon_{n,0}+\mu)}\sqrt{\frac{\mu}{\epsilon_{n,F}}}\Theta(\mu), \tag{14}$$

where $\Theta(x)$ is the Heaviside function. Its imaginary part reflects the decay of Cooper pairs into the two-particle continuum for $\mu>0$. However, for $\mu<0$, the imaginary part of d_n vanishes and the behavior of the order parameter is propagating, reflecting the presence of stable bound states. In addition, the coefficient of the fourth-order term in $\Lambda_n(q)$ is

$$b_n = \sum_{\mathbf{k}}\left(\frac{X_n}{4\xi^3_n(\mathbf{k})}-\frac{\beta Y_n}{8\xi^2_n(\mathbf{k})}\right)|\Gamma_n(\mathbf{k})|^4, \tag{15}$$

which is necessary to derive the time-dependent GL (TDGL) equations.

For completeness, we present the asymptotic forms of a_n, b_n, c_n, and d_n. The BCS limit is characterized by positive chemical potential with respect to the bottom of the lowest band $\mu>0$ and $\mu\approx\epsilon_{1,F}$. In this limit, we find $a_n=-g_{nn}+D_n[\ln(T/T_c)+\phi_-]$, $b_n=7D_n\zeta(3)/(8T_c^2\pi^2)$, $c_n=7\epsilon_{n,F}D_n\zeta(3)/(12T_c^2\pi^2)$, and $d_n=D_n[1/(4\epsilon_{n,F})+i/(8T_c)]$, where $\zeta(x)$ is the zeta function, and T_c is the physical critical temperature. On the other hand, the BEC limit is characterized by negative chemical potential with respect to the particle band $\mu<0$ and $\epsilon_{n,0}\gg|\mu|\gg T_c$. In this limit, we find $a_n=-g_{nn}-\pi D_n\epsilon_{n,0}/[2\sqrt{\epsilon_{n,F}}(\sqrt{|\mu|}+\sqrt{\epsilon_{n,0}})]$, $b_n=\pi D_n/(4|\mu|\sqrt{2|\mu|\epsilon_{n,F}})$, $c_n=\pi D_n/(16\sqrt{|\mu|\epsilon_{n,F}})$, and $d_n=\pi D_n/(8\sqrt{|\mu|\epsilon_{n,F}})$.

In order to obtain $\Omega_{\rm fluct}$, there are two contributions, one from the scattering states and the other from poles of $\mathbf{L}(q)$. The pole contribution dominates in the BEC limit. In this case, we evaluate $\det\mathbf{L}^{-1}(q)=0$ and find the poles

$$w_\pm(\mathbf{q}) = A_+ + B_+|\mathbf{q}|^2 \pm \sqrt{(A_- + B_-|\mathbf{q}|^2)^2 + \frac{g_{12}g_{21}}{d_1d_2}},$$

where $A_\pm=(a_1d_2\pm a_2d_1)/(2d_1d_2)$ and $B_\pm=(M_2d_2c_1\pm M_1d_1c_2)/(4M_1M_2d_1d_2)$. Notice that, when $J\to 0$, we recover the limit of uncoupled bands with $w_n(\mathbf{q})=a_n/d_n+|\mathbf{q}|^2c_n/(2M_nd_n)$. It is also illustrative to analyze the eigenvectors associated with these poles. In the $\mathbf{q}\to\mathbf{0}$ limit, the eigenvectors $[\Lambda^\dagger_1(0),\Lambda^\dagger_2(0)]=[g_{12},a_1-d_1w_\pm(0)]$ correspond to an in-phase mode for $w_+(\mathbf{q})$ and an out-of-phase mode for $w_-(\mathbf{q})$ when $J>0$; however, they correspond to an out-of-phase mode for $w_+(\mathbf{q})$ and an in-phase mode for $w_-(\mathbf{q})$ when $J<0$. Thus, we obtain $\Omega_{\rm fluct}=(1/\beta)\Sigma_{\pm,q}\ln\{\beta[iv_\ell-w(\mathbf{q})]\}$, which leads to

$$N_{\text{fluct}} = \sum_{\pm,\mathbf{q}} \frac{\partial w(\mathbf{q})}{\partial \mu} n_B[w(\mathbf{q})]. \quad (16)$$

In the BEC limit, $\partial w_{\pm}(\mathbf{q})/\partial\mu = 2$, and the poles can also be written as $w_{\pm}(\mathbf{q}) = -\mu_{B,\pm} + |\mathbf{q}|^2/(2M_{B,\pm})$, where $\mu_{B,\pm}$ is the chemical potential and $M_{B,\pm}$ is the mass of the corresponding bosons. In the case of identical bands ($M_1 = M_2 = M$) with zero offset ($\epsilon_D = 0$), $c_1 = c_2 = c$ and $d_1 = d_2 = d$, $\mu_{B,\pm} = -[a_1 + a_2 \pm \sqrt{(a_1 - a_2)^2 + 4g_{12}g_{21}}]/(2d)$ and $M_{B,\pm} = 2M$ in the BEC limit. Notice that the + bosons always condense first for any J (independent of its sign) since $\mu_{B,+} \to 0$ first. The familiar one-band results[4] are again recovered when $J \to 0$, leading to $\mu_{B,n} = -a_n/d_n = 2\mu_n - 1/(2M_n a_{nn}^2)$ and $M_{B,n} = M_n d_n/c_n = 2M_n$. Next, we analyze T_c in the strict BCS and BEC limits, where self-consistency equations are uncoupled, allowing analytical results.

B. Critical temperature

In the BCS limit, solutions to the order parameter equation Eq. (9) are

$$T_{c,\mp} = (8\epsilon_F/\pi)\exp[\gamma - 2 + \pi\sqrt{\epsilon_0/(4\epsilon_F)} - \phi_{\pm}],$$

while the number equation Eq. (8) leads to $\mu \approx \epsilon_F$. Here, we assumed $\epsilon_{1,F} \sim \epsilon_{2,F} = \epsilon_F$ and $\epsilon_{1,0} \sim \epsilon_{2,0} = \epsilon_0$. Notice that the physical critical temperature is $T_c = \max\{T_{c,+}, T_{c,-}\} = T_{c,+}$ for any J. The familiar one-band results are again recovered when $J \to 0$, leading to $T_{c,n} = (8\epsilon_{n,F}/\pi)\exp[\gamma - 2 + \pi\sqrt{\epsilon_{n,0}/(4\epsilon_{n,F})} - 1/\lambda_{nn}]$ for the order parameters and $\mu = \epsilon_{n,F}$ for the chemical potentials. The previous expression can be simplified using Eq. (7), leading to $T_{c,n} = (8\epsilon_{n,F}/\pi)\exp[\gamma - 2 + \pi/(2k_{n,F}a_{nn})]$.

On the other hand, in the BEC limit, the solution of the order parameter equation is

$$\mu_{\pm} = -\epsilon_0[\pi\sqrt{\epsilon_0/(4\epsilon_F)}/\phi_{\pm} - 1]^2,$$

while the number equation $\mathcal{N}/2 = \mathcal{N}_{B,+} + \mathcal{N}_{B,-}$ with $\mathcal{N}_{B,+} \gg \mathcal{N}_{B,-}$ leads to

$$T_{c,+} = (2\pi/M_{B,+})[\mathcal{N}_{B,+}/\zeta(3/2)]^{2/3},$$

since the + bosons condense first. Notice also that the physical critical temperature is $T_c = \max\{T_{c,+}, T_{c,-}\} = T_{c,+}$ for any J. Therefore, T_c grows continuously from an exponential dependence on interaction to a constant BEC temperature.

The familiar one-band results are again recovered when $J \to 0$, leading to $\mu_n = -\epsilon_{n,0}[\pi\lambda_{nn}\sqrt{\epsilon_{n,0}/(4\epsilon_{n,F})} - 1]^2$ for the chemical potentials,[3] and $T_{c,n} = (2\pi/M_{B,n})[\mathcal{N}_{B,n}/\zeta(3/2)]^{2/3}$ for the critical temperatures, where $\mathcal{N}_{B,n} = \mathcal{N}_n/2$ is the number and $M_{B,n} = 2M_n$ is the mass of the corresponding bosons. Using Eq. (7) and the condition $k_{n,0}a_{nn} \gg 1$, μ_n can be written in terms of the scattering lengths as $\mu_n = -1/(2M_n a_{nn}^2)$. In addition, $T_{c,n}$ can be expressed in terms of $\epsilon_{n,F}$ as $T_{c,n} = 0.218\epsilon_{n,F}$, as expected from the one-band calculations.[4]

C. TDGL equations

Next, we obtain the time-dependent Ginzburg-Landau equations for $T \approx T_c$. To study the evolution of the TDGL functional near T_c, we need to expand the effective action S_{eff} to fourth order in $\Lambda_n(x)$ around the saddle point order parameter $|\Delta_n| \to 0$ leading to

$$\begin{bmatrix} T_1 + b_1|\Lambda_1(x)|^2 & g_{12} \\ g_{21} & T_2 + b_2|\Lambda_2(x)|^2 \end{bmatrix} \begin{bmatrix} \Lambda_1(x) \\ \Lambda_2(x) \end{bmatrix} = 0 \quad (17)$$

in the real space $x = (\mathbf{x}, t)$ representation, where $T_n = a_n - c_n\nabla^2/(2M_n) - id_n\partial/\partial t$ The coefficient b_n of the nonlinear term given in Eq. (15) is always positive and guarantees the stability of the theory. In the BCS limit, Eq. (17) reduces to the coupled GL equations of two BCS-type superconductors. However, in the BEC limit, it is more illustrative to derive TDGL equations in the rotated basis of + and − bosons such that $\Lambda_1(x) = R_{11}\Phi_+(x) + R_{12}\Phi_-(x)$ and $\Lambda_2(x) = R_{21}\Phi_+(x) + R_{22}\Phi_-(x)$ where R_{nm} are the matrix elements of the inverse transformation matrix $\mathbf{R}$. Notice that the matrix $\mathbf{R}^{-1}$ is the unitary matrix that diagonalizes the linear part of the TDGL equations. In this basis, Eq. (17) reduces to generalized GP equations of $\Phi_+(x)$ and $\Phi_-(x)$ bosons

$$\begin{bmatrix} \tilde{T}_1 R_{11} + g_{12}R_{21} & 0 \\ 0 & g_{21}R_{12} + \tilde{T}_2 R_{22} \end{bmatrix} \begin{bmatrix} \Phi_+(x) \\ \Phi_-(x) \end{bmatrix} = 0, \quad (18)$$

where $\tilde{T}_1 = T_1 + b_1|R_{11}\Phi_+(x) + R_{12}\Phi_-(x)|^2$ and $\tilde{T}_2 = T_2 + b_2|R_{21}\Phi_+(x) + R_{22}\Phi_-(x)|^2$. The matrix elements R_{nm} are determined from the relations $[\tilde{T}_1 R_{12} + g_{12}R_{22}]\Phi_-(x) = 0$ and $[\tilde{T}_2 R_{21} + g_{21}R_{11}]\Phi_+(x) = 0$, and the unitarity condition $\mathbf{R}^{\dagger}\mathbf{R} = \mathbf{1}$. Notice that Eq. (18) shows explicitly terms coming from density-density interactions such as $U_{\pm\pm}|\Phi_{\pm}(x)|^2\Phi_{\pm}(x)$ or $U_{\pm\mp}|\Phi_{\pm}(x)|^2\Phi_{\mp}(x)$.

The familiar one-band results are again recovered when $J \to 0$ ($g_{12} = g_{21} \to 0$) leading to

$$\left[a_n + b_n|\Lambda_n(x)|^2 - \frac{c_n}{2M_n}\nabla^2 - id_n\frac{\partial}{\partial t}\right]\Lambda_n(x) = 0. \quad (19)$$

This expression reduces to the conventional TDGL equation upon rescaling of the pairing field as $\Psi_n(x) = \sqrt{b_n/D_n}\Lambda_n(x)$ in the BCS limit, while it reduces to the conventional GP equation upon rescaling of the pairing field as $\Psi_n(x) = \sqrt{d_n}\Lambda_n(x)$ in the BEC limit.[4]

V. ULTRACOLD FERMI GASES

We would like to emphasize that our results for identical bands ($M_1 = M_2 = M$) may be applicable to ultracold Fermi gases when four hyperfine states of a given type of atom are trapped. However, in atomic systems involving mixtures of two different alkali-metal atoms (e.g., ^{6}Li and ^{40}K), a more general two-band theory may be necessary to model future experiments. These more general two-band theories should allow pairing interactions between different Fermi atoms as well as the same Fermi atoms.

The phase diagram and the BCS to BEC evolution of superfluid mixtures involving only one hyperfine state (single pseudospin component) from each type of atom (A or B) and pairing only between different types of atoms (A-B

pairing) has been recently addressed.[28–30] These models rely on the assumption that the only important Feshbach resonance is that between A and B atoms. However, generalized models to describe Fermi mixtures should allow for the inclusion of pairing between the same species, as well as more than one hyperfine state (pseudospin component) of each species. For example, a model describing the mixture of one hyperfine state of Fermi atom A and one hyperfine state of Fermi atom B might need to allow for A-A, A-B, and B-B interactions, if A-A, A-B, and B-B Feshbach resonances turn out to be close to each other. In addition, it may be possible to trap two hyperfine states (pseudospin components) of Fermi atom A ($|A,1\rangle$ and $|A,2\rangle$) and two hyperfine states of Fermi atom B ($|B,1\rangle$ and $|B,2\rangle$). Thus, a model to describe this case may require interactions between fermions in all four states considered if Feshbach resonances between any two pairs of states are close to each other. Therefore, superfluidity in Fermi mixtures may be studied using a generalized multicomponent ("multiband") Hamiltonian

$$H = \sum_{n,\alpha,\mathbf{k}} \xi_{n\alpha}(\mathbf{k}) a^{\dagger}_{n\alpha}(\mathbf{k}) a_{n\alpha}(\mathbf{k}) - \sum_{n,m,\mathbf{k},\mathbf{k}'\mathbf{q}} V^{\alpha\beta\gamma\delta}_{nm}(\mathbf{k},\mathbf{k}') b^{\dagger}_{m\gamma;n\delta}(\mathbf{k}',\mathbf{q}) b_{n\alpha;m\beta}(\mathbf{k},\mathbf{q}),$$

where n and m label different types of Fermi atoms, $\alpha,\beta,\gamma,\delta$ label the different hyperfine states, and Einstein's notation is used to indicate summation over greek indices. Here, $\xi_{n\alpha}(\mathbf{k}) = \epsilon_{n\alpha}(\mathbf{k}) - \mu_{n\alpha}$, where $\epsilon_{n\alpha}(\mathbf{k}) = \varepsilon_{n\alpha,0} + k^2/(2M_n)$ is the kinetic energy ($\hbar = 1$), M_n is the corresponding mass of fermion type n, $\varepsilon_{n\alpha,0}$ is the reference energy for hyperfine state α, and $\mu_{n\alpha}$ is the chemical potential that fixes the number of fermions of type n in each hyperfine state α. Furthermore, the operator $a^{\dagger}_{n\alpha}(\mathbf{k})$ creates a Fermi atom of type n in hyperfine state α, while the operator $b^{\dagger}_{m\gamma;n\delta}(\mathbf{k},\mathbf{q}) = a^{\dagger}_{m\gamma}(\mathbf{k}+\mathbf{q}/2) a^{\dagger}_{n\delta}(-\mathbf{k}+\mathbf{q}/2)$ creates a pair of fermions with center of mass momentum $\mathbf{q}$ and relative momentum $2\mathbf{k}$. Notice that the interaction term above does not allow for the existence of Josephson coupling which would transform, for example, pairs of Fermi atoms of type A into pairs of Fermi atoms of type B, since these types of processes are unphysical.

VI. CONCLUSIONS

In conclusion, we analyzed the evolution of two-band superfluidity from the BCS to the BEC limit as a function of interaction strength at zero and finite temperatures. At zero temperature, we showed that a quantum phase transition occurs from a 0-phase to a π-phase state depending on the relative phase of the two order parameters, when the interband interaction is tuned from negative to positive values. We found that population imbalances between the two bands can be created by tuning intraband or interband interactions. In addition, we described the evolution of two undamped low-energy collective excitations corresponding to in-phase phonon (Goldstone) and out-of-phase exciton (finite-frequency) modes. Near the critical temperature, we derived the coupled time-dependent Ginzburg-Landau functional near T_c. We recovered the usual TDGL equations for BCS superfluids in the BCS limit, whereas in the BEC limit we recovered the coupled Gross-Pitaevskii equations for two types of weakly interacting bosons (tightly bound fermions).

ACKNOWLEDGMENTS

We thank the NSF (Grant No. DMR-0304380) for support.

[1] D. M. Eagles, Phys. Rev. **186**, 456 (1969).
[2] A. J. Leggett, in *Modern Trends in the Theory of Condensed Matter*, edited by A. Peralski and R. Przystawa (Springer-Verlag, Berlin, 1980).
[3] P. Nozieres and S. Schmitt-Rink, J. Low Temp. Phys. **59**, 195 (1985).
[4] C. A. R. Sá de Melo, M. Randeria, and J. R. Engelbrecht, Phys. Rev. Lett. **71**, 3202 (1993).
[5] J. R. Engelbrecht, M. Randeria, and C. A. R. Sá de Melo, Phys. Rev. B **55**, 15153 (1997).
[6] Y. Ohashi and A. Griffin, Phys. Rev. A **67**, 033603 (2003).
[7] A. Perali, P. Pieri, L. Pisani, and G. C. Strinati, Phys. Rev. Lett. **92**, 220404 (2004).
[8] K. E. Strecker, G. B. Partridge, and R. G. Hulet, Phys. Rev. Lett. **91**, 080406 (2003).
[9] C. A. Regal, M. Greiner, and D. S. Jin, Phys. Rev. Lett. **92**, 040403 (2004).
[10] M. Bartenstein, A. Altmeyer, S. Riedl, S. Jochim, C. Chin, J. H. Denschlag, and R. Grimm, Phys. Rev. Lett. **92**, 120401 (2004).
[11] J. Kinast, S. L. Hemmer, M. E. Gehm, A. Turlapov, and J. E. Thomas, Phys. Rev. Lett. **92**, 150402 (2004).
[12] T. Bourdel, L. Khaykovich, J. Cubizolles, J. Zhang, F. Chevy, M. Teichmann, L. Tarruell, S. J. J. M. F. Kokkelmans, and C. Salomon, Phys. Rev. Lett. **93**, 050401 (2004).
[13] M. W. Zwierlein, J. R. Abo-Shaeer, A. Schirotzek, C. H. Schunck, and W. Ketterle, Nature (London) **435**, 1047 (2005).
[14] G. B. Partridge, K. E. Strecker, R. I. Kamar, M. W. Jack, and R. G. Hulet, Phys. Rev. Lett. **95**, 020404 (2005).
[15] M. W. Zwierlein, A. Schirotzek, C. H. Schunck, and W. Ketterle, Science **311**, 492 (2006).
[16] G. B. Partridge, W. Lui, R. I. Kamar, Y. Liao, and R. G. Hulet, Science **311**, 503 (2006).
[17] Michael Köhl, Henning Moritz, Thilo Stöferle, Kenneth Günter, and Tilman Esslinger, Phys. Rev. Lett. **94**, 080403 (2005).
[18] H. Suhl, B. T. Matthias, and L. R. Walker, Phys. Rev. Lett. **3**, 552 (1959).
[19] M. Iavarone, G. Karapetrov, A. E. Koshelev, W. K. Kwok, G. W. Crabtree, D. G. Hinks, W. N. Kang, Eun-Mi Choi, Hyun Jung Kim, Hyeong-Jin Kim, and S. I. Lee, Phys. Rev. Lett. **89**, 187002 (2001).
[20] F. Bouquet, Y. Wang, I. Sheikin, T. Plackowski, A. Junod, S. Lee, and S. Tajima, Phys. Rev. Lett. **89**, 257001 (2002).
[21] S. Tsuda, T. Yokoya, Y. Takano, H. Kito, A. Matsushita, F. Yin, J. Itoh, H. Harima, and S. Shin, Phys. Rev. Lett. **91**,

127001 (2003).
[22] J. Geerk, R. Schneider, G. Linker, A. G. Zaitsev, R. Heid, K.-P. Bohnen, and H. v. Löhneysen, Phys. Rev. Lett. **94**, 227005 (2005).
[23] K. A. Parendo, K. H. Sarwa, B. Tan, A. Bhattacharya, M. Eblen-Zayas, N. E. Staley, and A. M. Goldman,Phys. Rev. Lett. **94**, 197004 (2005).
[24] A. J. Leggett, Prog. Theor. Phys. **36**, 901 (1966).
[25] M. Iskin and C. A. R. Sá de Melo, Phys. Rev. B **72**, 024512 (2005).
[26] J. Kinast, A. Turlapov, and J. E. Thomas, Phys. Rev. Lett. **94**, 170404 (2005).
[27] M. Bartenstein, A. Altmeyer, S. Riedl, S. Jochim, C. Chin, J. H. Denschlag, and R. Grimm, Phys. Rev. Lett. **92**, 203201 (2004).
[28] M. Iskin and C. A. R. Sá de Melo, , Phys. Rev. Lett. **97**, 100404 (2006).
[29] S.-T. Wu, C.-H. Pao, and S.-K. Yip, cond-mat/0604572 (unpublished).
[30] M. Iskin and C. A. R. Sá de Melo, cond-mat/0606624 (unpublished).